Genome-Wide Associations with Resistance to Bipolaris Leaf Spot (*Bipolaris oryzae* (Breda de Haan) Shoemaker) in a Northern Switchgrass Population (*Panicum virgatum*)

Kittikun Songsomboon[1*], Ryan Crawford[*], Jamie Crawford[*], Julie Hansen[*], Jaime Cummings[†], Neil Mattson[§], Gary Bergstrom[†], Donald Viands[*]

[*]Section of Plant Breeding and Genetics, School of Integrative Plant Science, Cornell University, Ithaca, NY 14853, USA

[†]Section of Plant Pathology and Plant-Microbe Biology, School of Integrative Plant Science, Cornell University, Ithaca, NY 14853, USA

[§]Section of Horticulture, School of Integrative Plant Science, Cornell University, Ithaca, NY 14853, USA

[1]Corresponding Author: K. Songsomboon, Email: ks899@cornell.edu Phone: +1 607 379 7332

RUNNING TITLE: Bipolaris leaf spot resistance in switchgrass

KEYWORDS:

Disease resistance, Bipolaris leaf spot, switchgrass, genome-wide association

[1]Corresponding Author: K. Songsomboon, Section of Plant Breeding and Genetics, School of Integrative Plant Science, Cornell University, Ithaca, NY 14853, USA.

Email: ks899@cornell.edu Phone: +1 607 379 7332

ABSTRACT

Switchgrass (*Panicum virgatum* L.), a northern native perennial grass, suffers from yield reduction from Bipolaris leaf spot caused by *Bipolaris oryzae* (Breda de Haan) Shoemaker. To determine the candidate resistant populations via multiple phenotyping approaches and identify potential resistance genes, single- and multi-trait genome-wide association studies were conducted in the northern switchgrass population. The disease resistance was evaluated from both natural and artificial inoculations. The natural inoculation from the field was evaluated in two locations – NY and PA, and artificial inoculations by leaf detachment and leaf disk assay were conducted and evaluated via both vision and image analysis. The most resistant population based on a combination of leaf detachment via image analysis (DTIA)-leaf disk via image analysis (DSIA)-mean from two locations was 'SW805' population. There were only four reliable GWAS results from various trait combinations in various subsets of genotypes including 1) full set of 479 genotypes with DTIA-DSIA-highest score from NY (MNY), 2) tetraploid with MNY, 3) lowland with DTIA-DSIA-MNY and highest score from PA (MPA), and 4) upland with leaf detachment via vision (DTVI)-MNY showing non-overlapping regions. Overall, the resistance genes were associated with 18 markers on chromosomes 1b, 2a, 2b, 3a, 3b, 5a, 5b, 6a, 7a, 7b, 8a, 9a, and 9b and accumulatively explained phenotypic variance of DSIA by 26.72% at the most and DTIA by 6.32% at the least. Within linkage disequilibrium of 20 kb, the potential resistance genes included genes encoding Myb, cytochrome P450, isocitrate lyase, E3 ubiquitin-protein ligase, mitogen-activated kinases, glutathione S-transferase, Birefringence-like 32, and ABC transporter.

INTRODUCTION

Switchgrass (*Panicum virgatum* L.) is a perennial biomass crop native to North America. Biomass and other agronomic traits have been the focus on improvement. Although many diseases have been reported to cause deleterious effects on yield, research on disease resistance, especially breeding for the resistance, is scarce. *Bipolaris oryzae* (Breda de Haan) Shoemaker (BO) is one of the major fungi causing Bipolaris leaf spot (BLS) in switchgrass that can reduce biomass by 70% (Fajolu, 2012). The approach for the disease management was to breed for improvement of resistance to BLS.

The natural distribution of switchgrass is broad latitudes across the USA east of the Rocky Mountains. By simple morphological differentiation, switchgrass can be separated into two groups of upland and lowland ecotypes. Upland ecotypes are well adapted to higher latitudes and higher drought tolerance whereas lowland ecotypes provide higher yield and require more water (Stroup et al., 2003). The more in-depth genetic diversity was revealed by Network-Based single nucleotide polymorphism (SNP) discovery protocol suggesting the differentiation of switchgrass group by isolation-by-ploidy, the migration from south to north, and the incidence of tetraploid upland from octaploid upland (Lu et al., 2013). Such a large diversity within switchgrass populations can provide a source of resistance.

Since BO is a necrotrophic pathogen, the interaction between switchgrass and the fungus was modelled as an inverse gene-for-gene model (Friesen et al., 2007). In general, the pathogen secretes necrotrophic effectors as host-selective toxins (HST) that interact with host sensitivity genes, resulting in a compatible susceptible

interaction to trigger host cell death (Friesen et al., 2008). Such an interaction is known as effector-triggered susceptibility (ETS). Interestingly, according to comparative genome study (Condon et al., 2013), BO does not produce any HST. Regardless of HST, BO produces ophiobolin A and B as a non-host-selective toxin (Xue et al., 2015) triggering many groups of proteins and enzymes such as reactive oxygen species (ROS) detoxification, protein phosphorylation, and ethylene production (Kim et al., 2014; Bockhaven et al., 2015).

Such an ETS interaction naturally removes the individuals with the necrotrophic effectors from the population. Breeding for the improvement of resistance to BLS can be done by eliminating susceptible genes from the population. However, the recurrent phenotypic selection for the resistance in ‘Shelter’ and ‘Cave-in-Rock’ for two cycles of selection did not provide any improvement (Songsomboon, 2018). Breeding for the resistance by various approaches, stages, and populations was suggested. Therefore, identification of resistant populations is a crucial step.

To accelerate breeding for disease resistance, genomics-assisted breeding is an important approach. Basically, it begins with gene identification, isolation, cloning, functional characterization, validation and utilization. There are two approaches to identify resistance genes: linkage mapping and genome-wide association studies (GWAS). Although GWAS cannot confirm the causal polymorphism, GWAS depends on linkage disequilibrium (LD) between the markers and the causal polymorphisms. With high allelic diversity and ancestral recombination events in the diversity panel, GWAS yields a finer resolution than linkage mapping (Yu and Buckler, 2006). The technique has been used to dissect flowering time in switchgrass (Grabowski et al.,

2017). Although GWAS has never been used to dissect disease resistance in switchgrass, it has successfully dissected resistance to leaf rust caused by *Puccinia triticina* Eriks., tan spot caused by *Pyrenophora tritici-repentis* (Die.) Shoemaker and stripe rust caused by *Puccinia striiformis* West. in wheat (*Triticum aestivum* L.) (Juliana et al., 2018). Despite no resistance genes identified in switchgrass, there were 13 SNP markers from quantitative trait loci (QTLs) linked with the resistance in rice (Sato et al., 2008, 2015). This study will provide the first dissection of the resistance to BLS in switchgrass.

The objectives were 1) to determine genotypes or populations from the northern switchgrass association panel that can be candidates for resistance to BLS, 2) to conduct a single- and multi-trait GWAS for resistance to BLS in the association panel via both natural and artificial inoculation, and 3) to explore the genes linked to the significant markers from the reliable GWAS model to determine potential candidate genes for resistance to BLS.

MATERIALS AND METHODS

Switchgrass in the Northern Association Panel

The switchgrass population used in this study has been developed for accelerating breeding progress especially for bioenergy traits at northern latitude (Lu et al., 2013; Lipka et al., 2014). The population consists of 479 genotypes from 66 populations representing the mostly upland northern population and some southern lowland population. It was initially planted in Ithaca, NY, in 2008 and then vegetatively cloned

and planted in a randomized, complete block design with three replicates in 0.9 m spaced planting in Ithaca, NY, and Philipsburg, PA, in 2016. No fungicide was applied to the field.

Disease evaluation and phenotype processing

Bipolaris leaf spot has been evaluated in both fields to determine the resistance in natural incidence and laboratory to minimize environmental effects on the resistance. Field evaluation was conducted in the same week in both locations in August 2017. Each plant was visually evaluated, the severity ranging from 0 to 5 as 0 = 0% BLS, 1= 1-10% BLS, 2= 11-25% BLS, 3= 26-50% 134 BLS, 4= 51-75% BLS, and 5= 76-100% of the leaf area with BLS. With artificial inoculation in the laboratory, disease severity was evaluated by leaf detachment and leaf disk assay by taking leaf samples from one replicate of genotypes in Ithaca, NY. In the leaf detachment assay, three healthy leaves were randomly selected from 30 centimeters below the top of the shoot to control the same stage of leaf development. The leaves were cut into five centimeters, washed with deionized water, placed in a pre-wet petri dish bedded with filter paper, kept cold in a cooler, and refrigerated overnight.

The inoculum was prepared from a subculture of a single conidium isolated from a ‘Carthage’ switchgrass leaf in the warm season biofuels field experiment in Ithaca, NY, by Katie Waxman. The day after collecting the detached leaf, the three-week-old plate was flooded, filtered via gauze, and the concentration adjusted to 10^5 conidia·ml^{-1} by hemocytometer with 2 drops of Tween-20 per 100 ml. An airbrush pressuring at 10 psi was used to spray inoculum on each dry-surfaced adaxial side of

the leaf in each plate. After letting the droplets of inoculum dry and firmly attach to the leaf surface, the plates were then sealed with a paraffin tape to maintain high moisture condition. The plates were kept at room temperature with 24-hour light for seven days (Figure 1). The disease evaluation was conducted by vision and image analysis software. Both evaluations were based on percentage of leaf covered with lesions. The evaluation by vision was from 0 to 100 % with 10% increment. Then each leaf was dried and scanned with a flatbed scanner (Canon CanoScan LiDE 700F) at a resolution of 1,200 dpi, and images were saved in .tiff format. Due to the limitation of laboratory space for the plates and labor in leaf collection, 85 to 200 genotypes were sampled in each set of the experiment, with some overlapping genotypes in one to three duplicated plates and additional non-inoculated plates. The leaf samplings were done weekly from May to June 2017. A total of seven sets of the experiment eventually covered all of 482 genotypes. Such an unbalanced design was handled with best linear unbiased prediction (BLUP) to extract random effect of the genotype by fitting the experiment factor as a fixed effect.

In the leaf disk evaluation, all of 479 genotypes were collected on the same day in August 2017 by cutting the same age leaves from each genotype and keeping them refrigerated overnight. On the next day, the leaves were washed with deionized water, surface dried, cut by keeping the midrib in the middle into an 8-mm disk, and placed on a water agar plate. There were 28 leaf disks in each plate, including four check disks (control and inoculated disks of resistant ‘SW43_09’ and susceptible ‘SW122_02’) and three replicated disks of eight genotypes (Figure 2). The inoculum was prepared the same way described above. For each leaf, two µL of inoculum was

dropped in the middle of the right side of the leaf. After letting the droplet dry, the plates were sealed with paraffin tape to keep high moisture and kept under 12-hour light at room temperature. The disease evaluation was conducted at seven dpi both by vision and image analysis software. The percent of leaf disk covered with lesions and necrotic tissue was assessed by a vision from 0 to 100 with ten increments. Also, on the same day, a photo was taken of each plate with a digital DSLR Cannon Rebel T6 DSLR camera with the resolution of 2644 x 3084 in .JPG.

Images from both leaf detachment and leaf disk assays were analyzed by using ImageJ macro at the setting provided in the Supplement file. In brief, each detached leaf or leaf disk was measured for total leaf area and total chlorosis lesion area (yellow and black area). Percentage of area covered with lesions was computed by dividing the total necrotic lesion area by total leaf area.

Package 'LME4' (Bates et al., 2015) in R was used to calculate Best Linear Unbiased Prediction (BLUPs) from various disease evaluations. For the field evaluation, BLUPs were computed based on each location separately and on the two locations combined using genotypes and replicates as random effects in each location model. BLUPs for the two locations combined were fitted genotype, replicates, locations, the interaction between genotypes and location, as random effects. In addition to generating BLUPs from field evaluation, the highest score, which is most severe symptoms observed from each location and two locations over replicates, were used due to successful QTLs of resistance to foliar symptoms caused by potato virus Y in autotetraploid potato (*Solanum tuberosum* L.) (Silva et al., 2017). For disease evaluations under laboratory condition, since all phenotypes were expressed as percentages

to leaf area, log transformation was performed before computing BLUPs. For the leaf detachment assay, BLUPs were computed with experiment, genotype, interaction between genotypes and experiment, plates within the experiment, and leaf replicates of genotypes as random effects. For the leaf disk assay, BLUPs were calculated with plates as a fixed effect and genotype, replicates within plates, and genotype within plates as random effects. Broad-sense heritability was estimated from variances in each model. Moreover, phenotypic correlations were computed between resistance to Bipolaris leaf spot to the other 20 morphological and biomass quality traits from Lipka et al. (2014), such as plant height, anthesis date, acid detergent lignin, minerals, ethanol·g^{-1} dry weight, etc.

Therefore, the resistance to BLS was evaluated via three approaches – leaf detachment, leaf disk, and field evaluation – providing phenotyped traits including BLUPs of detached leaf percent lesion via vision and image analysis (DTVI and DTIA), BLUPs of leaf disk percent lesion via vision and image analysis (DSVI and DSIA), BLUPs of field evaluation from two locations, NY and PA (BTL, BNY, and BPA), highest score from two locations, NY and PA (MTL, MNY, and MPA).

Genotyping, linkage disequilibrium analysis, and population structure

HAPMAP v.1 set from Evans et al. (2015) provided 1,377,841 single-nucleotide polymorphisms covering 38,654 genic regions. In short, DNA of each genotype was processed via exome-capture using the Roch-Nimblegen switchgrass exome-capture probe set (Evans et al., 2014) and DNA sequencing. The sequences were aligned

to the *P. virgatum* genome assembly v.1.1 (*P. virgatum* v.1.1, DOE-JGI, http://phytozome.jgi.doe.gov/) for SNP discovery. In this calling, SNPs were required to be bi-allelic, sequenced in all samples, be monomorphic in at least two samples, and have more than 5X coverage in more than 95% of the samples. At each SNP, the genotype dosages ranged from zero to two copies of minor alleles and can be nonintegers by using EM algorithm (Martin et al., 2010). Naturally, the switchgrass association panel includes allopolyploid switchgrass: tetraploids (4x), octoploids (8x) and hexaploids (6x). It is challenging to perform GWAS with polyploid models. In this study, we modelled them under the assumption of disomic inheritance similar to the study of GWAS of flowering time in Grabowski et al. (2017). This was because tetraploid switchgrass was confirmed to show disomic inheritance (Okada et al., 2010). Although octaploid switchgrass had four copies of each homologous chromosome, which was difficult to precisely determine heterozygous genotypes, the disomic segregation was used for the model with the caution of the increasing standard error of estimates in GWAS. Moreover, linkage disequilibrium (LD) was computed via '-r2' tag in PLINK as r^2 between all SNPs within 1 MB and recorded all values (Purcell et al., 2007). Principle component analysis was used to evaluate the population structure via TASSEL v.5 (Trait Analysis by aSSociation Evolution and Linkage) (Bradbury et al., 2007)

Genome-wide association studies

Genome-wide Efficient Mixed Model Association (GEMMA) (Zhou and Stephens, 2012) was used to implement a multivariate linear mixed model for GWAS

of single- and multiple-phenotyping approaches for resistance to BLS. Kinship was included as a random effect. Also, the first three principal components (PCs) were included as fixed covariates. Although the results of Bayesian information criterion resulted in no improvement of the GWAS model with PC inclusion (Lipka et al., 2013), the inclusion of PCs helped to improve the QQ-plot closer to the theoretical QQ-plot for this resistance to BLS. The GWAS was conducted in five groups including all of 479, lowland, upland, tetraploid (4X), and octaploid (8X) genotypes to determine if there were any SNPs linked to specific switchgrass population. Minor allele frequency (MAF) at 0.05 was used to filter the minor alleles. To correct multiple testing, false discovery rate (FDR) was used for a cut-off value at 0.1. The significant markers then were used to determine candidate genes linked to them within the range of LD and search in JBrowse in *P. virgatum* v.1.1 in Phytozome (e.g., if the position of the marker was 77345950 on chromosome 2a and LD was 20 kb, "Chr02a:77335950..77355950" was used). In case that the candidate gene was not fully aligned within that LD range, we considered the gene as a candidate if 80% of its length was within the LD range. Since some of SNPs' positions could not be aligned to the *P. virgatum* genome assembly v.1.1, they were grouped as U1-U4 chromosome and were excluded from determining the candidate genes.

Candidate genes based on resistance in rice

Since *B. oryzae* is one of the major pathogens in rice (*Oryza sativa*), major resistant QTLs have been identified in recombinant inbred lines (RILs) and double haploids (DH) by using restriction fragment length polymorphism (RFLP), simple-

sequence repeat (SSR) markers, and sequence- tagged site (STS) (Sato et al., 2008, 2015; Katara et al., 2010). Three major QTLs in Chromosomes 1, 4 and 11 were then studied further in near-isogenic lines (NILs) and 13 SNP markers linked with the resistance (Sato et al., 2015). The NILs are BC3F5 between indica 'Tadukan' (resistance) and temperate japonica 'Koshihikari' (susceptible). According to GWAS in rice, linkage disequilibrium (LD) are ~ 100 kb in indica and ~200 kb temperate in japonica (Zhao et al., 2011). Thus, in this study, the candidate resistance genes were screened from 200 kb around the 13 SNPs from *Oryza sativa* genome assembly v.7.0 (*Oryza sativa* v.7.0, DOE-JGI, http://phytozome.jgi.doe.gov/). The candidate genes from rice are listed in the table S1. The sequences of these candidate genes were used to identify potential homologs in switchgrass by using the BLASTP tool on Phytozome (Goodstein et al., 2012).

RESULTS

Phenotyping and correlation between traits

The results from leaf detachment showed that 'ECS.6' was the most resistant population (DTVI 24% and DTIA 8%) and 'SW115' was the most susceptible population (DTVI 81% and DTIA 60%) (Table S2). However, when comparing each genotype, 'SW788.05' was the most resistant genotype (DTVI 6% and DTIA 2%) whereas 'SW63.05' was the most susceptible genotype (Table S3). The result from the leaf disk assay showed that 'SW803' was the most resistant population (DSVI 20% and DSIA 48%) and 'SW38' was the most susceptible population (DSVI 98% and DSIA

99%). In the genotype-based comparison, ‘High Tide.02’ showed the most resistance (DSVI 10% and DSIA 11%), but the most susceptible were 81 genotypes with DSVI 100% and DSIA 100%. In the field evaluation based on the mean of the severity score (0 to 5) from two locations, ‘Shelter’ appeared to be the most resistant population (0.44) and ‘SW787’ was the most susceptible. However, when considering each location, different populations performed differently due to high GxE effect. In NY, SW803 showed the most resistant population (0.22) and SW787 appeared to be the most susceptible one (3.0). Whereas, in PA, Shelter appeared to be the most resistant one (0.33) and Pathfinder appeared to be the most susceptible population (2.9). As Silva et al. (2017) phenotyped potato tuber necrotic ringspot disease by using the highest score for the disease evaluation across replicates to be able to review significant QTLs, the highest score for BLS was considered to be used in this study also. At the two locations, ‘SW123’, ‘SW33’, ‘SW793’, ‘SW781’, High Tide, and Timber had the lowest MTL at 3 (resistant), and 41 populations had the highest MTL at 5 (susceptible). In NY, SW123, SW128 and ‘ECS.6’ had the lowest MNY at 2, and 32 populations had the highest MNY at 5. In PA, ‘SW115’, ‘SW802’, ‘SW31’ and ‘SW43’ had the lowest MPA at 2, and 19 populations had the highest MPA at 5. The most resistant and susceptible genotypes in each phenotyping approach are listed in the Table S3. Based on artificial inoculations, both the leaf detachment and the leaf disk assay suggested that the lowland ecotypes (DTVI 43%, DTIA 21%, DSVI 43% and DSIA 70%) appeared to be more resistant than upland ecotypes (DTVI 61%, DTIA 39%, DSVI 67% and DSIA 89%); however, the field evaluation of means between two locations did not show the same trend (Figure S1).

Although each trait from different phenotyping approaches had significantly moderate to high broad-sense heritability (H) (Table 1), H of severity from two locations was zero. This was suggested by the different trends of the mean of severity from two locations, NY and PA (Figure S2). Due to zero heritability, the BTL was zero and cannot be used for conducting GWAS. The different trends were not only present in the field evaluation, the other phenotyping approaches yielded different trend of resistance as suggested by the trends of DTIA, DSIA and mean from two locations and correlation among the traits (Figure S2 and Figure 3). For example, from 479 genotypes, 'KY1625_07' ranked 27 from DTIA but ranked 260 in DSIA, and 100 in mean from two locations. Such differences led to low correlation among approaches such that the r^2 between DTIA and DSIA was only 0.1 and between DTIA and mean of two locations was 0.03 (Figure 3). In contrast to these low correlations, there were high correlations in DTVI-DTIA (r^2 = 0.84) and DSVI-DSIA (r^2 = 0.85). There was no BLS resistance trait correlating to other agronomic or biomass quality traits (Figure S3).

Linkage disequilibrium and principal component analysis

To determine the gene interval that potentially linked to the significant markers from GWAS, linkage disequilibrium (LD) decay was estimated by plotting the allele frequency correlations (R^2) against the physical distance in base pairs (Figure 4). In the full set of 479 genotypes, the LD decayed sharply within 20 kb and reached a plateau background within 50 kb. The other groups of 4X, 8X, lowland and upland genotypes showed a similar pattern of the

LD despite being slightly different in an 8X group. Therefore, in this study, we focused on genes within the 20 kb from the significant SNPs.

Based on the principal component analysis, there was a strong population structure in this association panel (Figure 5). From PC1 and PC2, upland and lowland ecotypes were apart from each other. Also, within the lowland ecotype, the latitude of lowland can be distinguished to lowland north and south groups. The separation of upland ecotype can also be noticed in PC1 and PC3 in that the upland north was grouped apart from the other upland. Besides ecotypes, ploidy level can be differentiated into groups. Both lowland north and south, and upland north genotypes were tetraploid (4X) while the upland east and upland west genotypes were octaploid (8X). In total, PC1, PC2, and PC3 explained the variance due to the population of 15.03%.

Genome-wide association mapping

As we conducted GWAS with five subsets of genotypes including 479 upland, lowland, 4X and 8X to multiple combinations of assessing resistance to BLS via many phenotyping approaches, almost all the combinations for GWAS did not provide reliable results based on flat or inflated QQ-plots. In the full set of 479 genotypes, single traits from artificial inoculation via either leaf detachment or leaf disk assay with vision or image analysis (DTVI, DTIA, DSVI, and DSIA) provided reliable GWAS results based on inflated QQ-plot (Figure S4). Although DSIA showed the best QQ-plot (Figure S4d), the convex head and inflated tail of -log(P-value) suggested confounding of the association analysis. The single-trait GWAS of field evaluations (MTL, MNY, MPA, BNY, BPA, mean of two locations, mean of NY, and mean of PA) did not yield any reliable association analysis (Figure S5). The combination of two traits from artificial inoculations yielded better QQ-plots, but they still showed unreliable QQ-plots with a convex head and early inflation in the middle of the plot. Among the two-trait GWAS, DTIA-DSIA analysis provided the better GWAS with the QQ-plot that delayed the inflated tail from -log(P-value) of 2 to about 2.5. To improve the association analysis, the GWASs were then conducted with the combination of two artificial inoculations (DTIA-DSIA) with field evaluations. The only three-trait combination that provided reliable GWAS was DTIA-DSIA-MNY due to the QQ-plot with the expected distribution (Figure S6d).

In a tetraploid group, the same three-trait combination of DTIA-DSIA-MNY did not provide the better GWAS than did MNY alone (Figure S7c, d). Among all the trait combinations in the tetraploids, MNY provided the best association analysis with the expected distribution. However, none of the GWAS octaploid group provided significant GWAS with reliable QQ-plots. In the lowland group, the most reliable GWAS was from the combination of

DTIA-DSIA-MNY-MPA (Figure S8d). Interestingly, in the upland group, none of the image analysis traits of DTIA and DSIA provided a reliable GWAS. The only nearly reliable single-trait GWAS in the upland group was DTVI with the convex line in the middle of the QQ-plot (Figure S9a). The two-trait combination of DTVI-MNY provided the most reliable GWAS with the expected QQ-plot (Figure S9c). In contrast to the full set of 479 genotypes, the inclusion of the trait from the leaf disk assay did not improve the analysis (Figure S9d).

In this study, therefore, we focused on four reliable GWAS analyses including 479-DTIA-DSIA-MNY, 4X-MNY, low-DTIA-DSIA-MNY-MPA, and up-DTVI-MNY (Figure 6). However, there was no overlapping region associated with the resistance among the four GWAS analyses (Table 2). Accumulatively, when considering phenotypic variance explained (PVE) by all 18 significant SNP markers for each trait, PVE of DSIA was the highest at 26.72% and PVE of DTIA was the lowest at 6.32% (Table 3). In 479-DTIA-DSIA-MNY, the significant markers were on chromosomes 2b, 6a, 7b, 9a, and 9b. The most significant marker on chromosome 2a was snp680175 followed by snp151084. Only snp359167 was the significant marker on chromosome 6a. The most significant marker on chromosome 7b was snp938364 followed by snp933838. The most significant marker on chromosome 9a was snp469523 followed by snp465249. The snp1003871 was the only significant marker on chromosome 9b. These eight SNP markers explained phenotypic variances for DTIA, DSIA and MNY of 2.1, 24.28, and 5.27%, respectively (Table S4). In 4X-MNY, there were only two significant markers snp316732 on chromosome 5a and snp444058 on chromosome 8a, accumulatively explaining 1.58% in MNY. In low-DTIA-DSIA-MNY-MPA, the significant markers were on chromosomes 1b, 3a, 3b and 5b. Only snp594527 was the significant marker on chromosome 1b. Also, snp197006 was the only significant marker on chromosome 3a, and

snp732235 was the only one on chromosome 3b. The most significant marker on chromosome 5b was snp791318 followed by snp791375. These five SNP markers explained phenotypic variances for DTIA, DSIA, MNY, and MPA of 2.41, 8.31, 6.86, and 32.48%, respectively. In up-DTVI-MNY, the significant markers were on only chromosome 7a, in which snp411995 was the most significant marker, followed by snp411929 and snp412960. Among these markers, only snp938364, on chromosome 7b from 479-DTIA-DSIA-MNY, was linked with two genes: Pavir.Gb01488.1 and Pavir.Gb01488.2. These two were the only genes that overlapped with LOC_Os04g39430.1, one of the potential candidate genes for resistance to BLS in rice on chromosome 4 from AE11005627 marker (Table S1). Also, these three SNP markers explained phenotypic variances for DTVI and MNY of 7.19 and 0.27%, respectively. The PVEs of each SNP in each subgroup and each trait are reported in Table S5.

From the QTLs study of Sato et al. (2015), the candidate resistance genes in rice were reported to be on three chromosomes with 13 SNPs markers within the LD of 200 kb (Table S1). There were 278 genes linked to these markers. Among them, 172 genes were annotated with 134 biological functions. There were 106 non-annotated genes. The most frequent biological functions were Leucine-rich repeat family protein (6), peroxidase precursor (6), transposon protein (6), nucleotide binding sites – leucine rice repeats (NBS-LRR) type disease resistance protein (5), MYB family transcription factor (3), dirigent (2), fasciclin domain-containing protein (2), flavin monooxygenase (2), and heavy metal associated domain (2).

DISCUSSION

The most resistant population for improvement of resistance to BLS

Since the various phenotyping approaches yielded various resistant populations, it was challenging to determine the most resistant candidates for further breeding. Based on field evaluation, BLUPs from two locations were zero due to zero broad-sense heritability. This indicated huge GxE effects between two locations. If the mean of field scores were used, the upland Shelter should be considered the most resistant population across two locations with a mean of 0.44. The high resistance of Shelter from field evaluation might explain the reason in Songsomboon (2018) that it cannot be improved for resistance to BLS in recurrent phenotypic selection in seedlings. However, the most susceptible SW787 had the mean score only 2.33. This suggested the low natural inoculation in 2017 which was not conducive to severe disease development. When comparing each location, the most resistant population in NY was SW803 at 0.22, but it was almost the most susceptible population in PA at 2.11. Therefore, this variation needs to be confirmed with more replicates, years, and locations.

To lessen the GxE effect on the BLS, artificial inoculation was conducted in the laboratory. In the leaf detachment assay, due to the limitation of sampling, a whole set of 479 genotypes cannot be tested at the same time. The experiment was separated into seven overlapping sets. However, there was significant variation among sets. Such a variation can occur from the different age of each genotype in the same sampling time. Although the same stage of leaves was sampled at 30 centimeters from the top, variation existed among leaves from the same plant. To handle the variation among sets, BLUPs were used by fitting the effect from the set as a fixed effect. Another artificial inoculation was leaf disk assay, without limitation of the size, the whole set of 479 genotypes was sampled at the same time with resistant and susceptible checks in each plate. Although a small effect of plates existed, BLUPs was fitted by considering plates as a fixed effect. Both artificial inoculations were evaluated via vision

and image analysis. Although vision and image analysis results were highly correlated, they yielded a different result from association analysis. Image analysis, however, provided a more significant analysis. It could be explained by the more refined data from image analysis with decimals than vision analysis (which grouped into ten increments). Moreover, the image analysis is better regarding repeatability and reanalysis (Stewart and McDonald, 2014). For the sake of comparison for the most resistant population, mean of percent lesion from image analysis was considered. In the leaf detachment approach, the most resistant population from DTIA was ECS.6 at 8%, but the population appeared very susceptible from DSIA at 94%. In leaf disk assay, the most resistant population from DSIA was SW803 and SW793. These confirmed the low correlation among all three disease evaluation approaches. Regardless of low correlations, SW805 was the most resistant population across the mean of two locations, DTIA, and DSIA, 10% and 56% resistance, respectively, with mean of 0.78.

The improvement of multi-trait GWAS from single trait GWAS

Although all single traits from a different phenotype approach had moderate to high heritability, none of them provided reliable GWAS based on QQ-plots that were not distributed as expected from theory. This unreliability can be explained by the high density of markers with high collinearity between markers, and too small population size giving the low power detection (Muir, 2007). The combination of the traits for resistance to BLS from different approaches helped improve the association analysis power (Guo et al., 2017). However, the addition of traits did not always improve the analysis. In the tetraploid groups, for example, only MNY yielded the most reliable GWAS. These suggested significant markers linked with the specific location. The spatial markers of simple sequence repeats (SSRs) in QTLs were also reported in resistance to BLS in rice (Katara et al., 2010). None of the reliable

GWAS provides the same significant regions linked with the resistance to BLS. As those reliable GWASs were from a different subset of the association panel, it suggested different resistance allele distribution in the subgroups. It also suggests the multifaceted defense mechanism to BLS.

Despite the improvement of multi-trait GWAS over single-trait GWAS, 18 SNP markers can explain the phenotypic variance ranging from only 6.32 to 26.72% among DTVI, DTIA, DSIA, MNY and MPA. The low PVE from GWAS is a common phenomenon and generally caused by missing heritability and can be improved by more genomic imputation and implementation of a large-scale next-generation sequence data (Fan and Song, 2016).

Moreover, each genotype group can show reliable GWAS with specific traits. For example, the upland group only provided the reliable GWAS with DTVI-MNY, whereas the full set of 479 genotypes provided the best fit GWAS with DTIA-DSIA-MNY. To further study resistance to BLS in switchgrass populations, single-trait GWAS is not suggested due to the low power of determining significant markers. Multi-trait GWAS from both artificial and natural inoculation were suggested to improve the power. However, such an improvement cannot be applied to the octaploid population due to the uncertainty in differentiating heterozygote genotypes. The model for octaploid should be applied to the population instead of the diploid model to detect associations.

Dissecting resistance to BLS

As mentioned previously, none of the significant markers overlapped across reliable GWASs from different groups. Although this suggested the different distribution of resistance genes in different subgroups from the association panel, we considered the biological functions for the resistance over the fixation of the alleles in each population. In the full set, on chromosome 2b, Pavir.Ba03861.1 was predicted to function as a copper transport protein and as an antioxidant protein 1 (ATOX1). There was no study to confirm the function of this gene related to any plant disease resistance, but its antioxidant capacity may help handle ROS from the interaction between fungal effectors and plant response. Pavir.Bb02195.1 and Pavir.Bb02196.1 encoded RING-type E3 ubiquitin-protein ligase and RBR family ring finger, respectively, which collaboratively regulates cell death and immunity in rice (Smit and Sixma, 2014; You et al., 2016). On chromosome 6b, Pavir.Fa00433.1 encoded for the EMSY N-terminal (ENT) domain, which is important to mediate the race-specific NLR gene resistance to *Peronospora parasitica* (*RPP7*) gene in *Arabidopsis thaliana* (Tsuchiya and Eulgem, 2011). Moreover, Pavir.Fa00434.1 encoded the Myb-like DNA-binding domain. This gene was confirmed to control many biological functions like biotic and abiotic stress, development, defense, etc. in many organisms (Ambawat et al., 2013). In rice, the *MYB* gene controls Jasmonic acid (JA) against rice blast fungus: *Pyricularia greisea* (Lee et al., 2001). In Arabidopsis interaction with necrotrophic *Alternaria brassicicola*, the response to JA was the upregulated plant defensin protein (*Pdf*) gene. This gene was negatively controlled by the heat stress transcription factor B-1 encoded from Pavir.Fa00437.1 (Kumar et al., 2009). The most interesting region linked with significant markers was on chromosome 7b since Pavir.Gb01488.1 and Pavir.Gb01488.2 were the only genes that overlapped with the BLAST

result of the resistance to BLS in rice. These two genes encoded for cytochromes P450, which involved diverse oxidation reactions and triterpene synthesis (Geisler et al.,). The most well-known triterpene against fungal disease was Avenacins in oat (*Avena* spp.). Also, Pavir.Gb01298.1 encoded for the polyadenylate-binding protein. Polyadenylation is an important process to mediate transposon slicing of the RPP7 gene in Arabidopsis (Tsuchiya and Eulgem, 2013). Pavir.Gb01299.1 encoded for Isocitrate lyase, which was naturally a component of the glyoxylate cycle and was required for the pathogenicity of ascomycete *Leptosphaeria maculans*, causing blackleg disease of canola (*Brassica napus*) (Idnurm and Howlett, 2002). On chromosome 9a, the most interesting gene was Pavir.Ia00351.1 encoding mitogen-activated kinase (MAP). The mediation of the MAP has confirmed the activation of expression of ethylene (ET), JA, and salicylic acid (SA) in the response to both abiotic and biotic stress in Arabidopsis (Brader et al., 2007). Moreover, Pavir.Ia00174.1 encoded trichome Birefringence-like protein responsible for xylan acetylation in rice, which conferred the resistance to bacterial leaf blight (Gao et al., 2017). On chromosome 9b, Pavir.Ib01315.1, Pavir.Ib01315.2, Pavir.Ib01317.1 encoded glutathione S-transferase (GST) which was an important enzyme in redox reactions in cells. Glutathione was the key compound in the signaling process to trigger plant resistance to pathogens (Dubreuil-Maurizi and Poinssot, 2012).

In 4X-MNY, on chromosome 5a, Pavir.Ea02827.1, encoding Actinidain, cysteine protease and Cathepsin propeptide inhibitor, was directly involved in programmed cell death in the plant (Solomon et al., 1999). Additionally, Pavir.Ea02828.1 encoded DEAD/DEAH box helicase, which showed the up-regulation of defense-related signals like SA and JA and conferred the resistance again rice blast fungus *Manaporthe grisea* (Li et al., 2008). On chromosome 8a, Pavir.Ha00272.1 encoded for auxilin/cyclin G-associated kinase (GAK). Besides

relating to the kinase signal group conferring innate immunity, auxilin-like protein itself was confirmed to induce necrotic lesion and confer resistance to *Xanthomonas oryzae* pv. Oryzae (Xoo) (Park et al., 2017).

In low-DTIA-DSIA-MNY-MPA, on chromosome 1b, Pavir.Ab01193.1, Pavir.Ab01193.2, and Pavir.Ab01193.3 encoded ginkbilobin-2. This protein was purified from *Ginkgo biloba* seeds. It is cysteine-rich receptor-like kinase that confirmed the functions of salt stress and antifungal activity (Sawano et al., 2007; Miyakawa et al., 2009). On chromosome 3b, Pavir.Ca02197.1 encodedf ATP-binding cassette (ABC) transporter. There are many subgroups of ABC. In Arabidopsis, the mutant lacking the ABC transporter of PENETRATION3/ PLEIOTROPIC DRUG RESISTANCE8 (PEN3/PDR8) conferred nonhost susceptibility to *Blumeria graminis* f. sp hordei., suggesting that the ABC transporter was involved in exporting secreted toxins from the fungus and fungal suppressor from the host (Stein et al., 2006). Also, in wheat, the ABC suggested the exportation of mycotoxin conferring resistance to Fusarium head blight (Walter et al., 2015). On chromosome 3b, Pavir.Cb01412.1 encoded copines, which were diverse protein classes related to calcium-, phospholipid-binding function. The study in Arabidopsis suggested that copines acted as suppressors of defense responses in hypersensitive cell death defense against *Pseudomonas syringae* pv *tomato* (Jambunathan and McNellis, 2003). On chromosome 5b, Pavir.Eb00172.1 encoded serine/threonine protein kinase (STPK) which were known to be candidates conferring disease resistance in wheat to tan spot (Juliana et al., 2018) and Arabidopsis to flagellin bacteria (Gómez-Gómez and Boller, 2000). Pavir.Eb00173.1 encoded BED zing finger which was classed as NBS-LRR, which played an important role in effector-triggered immunity (ETI). The zing finger domains suggested the broad-spectrum nature of rice blast resistance gene

Pi54 (Gupta et al., 2012). Pavir.Eb00177.1 encoded chloroplastic membrane protein, which also can involve mediating ROS from avirulent pathogen invasion (Yaeno et al., 2004).

In up-DTVI-MNY, although there was only one significant peak of markers on chromosome 7, it was unlikely to conclude that there was an R gene in this chromosome due to multiple significant SNPs with diverse roles. Pavir.Ga00855.1 encoded STPK similarly to Pavir.Eb00172.1 on chromosome 5. Pavir.Ga00857.1 and Pavir.Ga00858.1encoded for transporter proteins like Pavir.Ca02197.1 on chromosome 3b. Lastly, Pavir.Ga00912.1 encoded WD40 repeat family protein. Although there was no study directly with disease resistance, WD40 is involved in many biosynthesis pathways such as Transparent Testa2, which is a Myb transcription factor related to the resistance as explained earlier, and flavonoid biosynthesis for antioxidation handling ROS.

Although these candidate genes from the switchgrass association panel shared some of the functions from candidate genes from rice resistance to BLS, some of the potential functions conferring resistance were still missing such as dirigent protein, peroxidase, and Mlo-like protein. Dirigent protein conferred resistance by lignin and lignan synthesis (Ralph et al., 2006). The lignin synthesis was expected to relate with resistance to BLS by strengthening cell walls (Dallagnol et al., 2013). However, since none of the resistance traits for BLS correlated with lignin, the missing dirigent protein from detection can be expected. Peroxidase also played an important role in Pathogen-associated molecular pattern-triggered immunity (PTI) (Mammarella et al., 2015). This was unexpected due to the high involvement of ROS in the infection of BO (Antonious and Jawhar, 2013). Mlo was identified to provide broad resistance to powdery mildew in barley (Jorgensen, 1992). More powerful model and finer phenotype combinations were needed to clarify these missing candidates.

CONCLUSIONS AND POTENTIAL APPLICATIONS

In conclusion, the resistance to BLS yielded differently based on different phenotyping approaches, with low correlations suggesting that resistance was sensitive to phenotyping methods in different conditions. Although it is difficult to standardize the phenotyping approach that can take account all conditions, finer and more powerful phenotyping of the resistance is still needed. As such, to the best of our phenotyping combination, SW805 should be considered the most resistant population. Based on obtained phenotypes, our multi-trait GWAS with four subsets from 479 genotypes have a handful of markers that can be considered as potential candidate genes related to resistance to BLS with reasonable biological functions. Nevertheless, one needs to be prudent regarding the utilization of these markers. Due to low correlations between resistance to BLS from different phenotyping approaches, the combinations of the trait in a different subgroup of genotypes provided no significant overlapping regions. The application of these markers cannot be directly transferred for genomics-assisted selection without validation to the choices of phenotyping approaches in new populations.

When considering biological functions from the GWAS regardless of subgroup and trait combinations, the defense mechanisms against BLS are complicated and multifaceted, probably controlled by multiple small-effect alleles. Most of the responses involved ETI via signaling kinases and NBS-LRR. Moreover, basal defense mechanism and PTI mostly via oxidative stress also played an important role in response to BLS. Despite missing expected candidate functions and only one overlapping gene for resistance to BLS in rice, most of the genes from these GWASs in switchgrass encode proteins overlapping with genes in rice. To my knowledge, this was first research to dissect the resistance to BLS in switchgrass. With the

current power of detection within the population, multi-trait GWAS can provide functional insight into the resistance within multiple subsets of genotypes.

ACKNOWLEDGEMENTS

The project is supported by PhD funding from the Development and Promotion of Science and Technology Talents Project (DPST), the Royal Thai Government. The northern switchgrass association panel and its HAPMAP data were provided by Dr. Michael Casler and Dr. Paul Grabowski from US Dairy Farage Research Center, USDA-ARS. The genome-wide association analysis with multiple traits was consulted by Dr. Deniz Akdemir. Visual and digital disease evaluations were guided by Dr. Shawn Kenaley and Dr. Ethan Stewart.

LITERATURE CITED

Ambawat, S., P. Sharma, N.R. Yadav, and R.C. Yadav. 2013. MYB transcription factor genes as regulators for plant responses: an overview. Physiol. Mol. Biol. Plants 19(3): 307–21.

Antonious, A. D., & Jawhar, M. 2013. Proteome analysis of the susceptible barley-Cochliobolus sativus interaction. Research in Biotechnology. 4(2).

Bates, D., Mächler, M., Bolker, B., & Walker, S. 2014. Fitting linear mixed-effects models using lme4. arXiv preprint arXiv:1406.5823.

Bockhaven, J. V., Spíchal, L., Novák, O., Strnad, M., Asano, T., Kikuchi, S., & De Vleesschauwer, D. 2015. Silicon induces resistance to the brown spot fungus *Cochliobolus miyabeanus* by preventing the pathogen from hijacking the rice ethylene pathway. New Phytologist. 206(2): 761-773.

Bradbury, P.J., Z. Zhang, D.E. Kroon, T.M. Casstevens, Y. Ramdoss, and E.S. Buckler. 2007. TASSEL: software for association mapping of complex traits in diverse samples. 23(19): 2633–2635.

Brader, G., A. Djamei, M. Teige, E.T. Palva, and H. Hirt. 2007. The MAP kinase kinase MKK2 affects disease resistance in arabidopsis. 20(510): 589–596.

Condon, B. J., Leng, Y., Wu, D., Bushley, K. E., Ohm, R. A., Otillar, R., & Xue, C. 2013. Comparative genome structure, secondary metabolite, and effector coding capacity across Cochliobolus pathogens. PLoS Genetics, 9(1), e1003233.

Dallagnol, L., F. Rodrigues, and M. Mielli. 2013. Silicon improves the emergence and sanity of rice seedlings obtained from seeds infected with Bipolaris oryzae. Trop. Plant Pathol. 38(6): 478–484.

Dubreuil-Maurizi, C., and B. Poinssot. 2012. Role of glutathione in plant signaling under biotic stress. Plant Signal. Behav. 7(2): 210–2.

Evans, J., E. Crisovan, K. Barry, C. Daum, J. Jenkins, G. Kunde-Ramamoorthy, A. Nandety, C.Y. Ngan, B. Vaillancourt, C.-L. Wei, J. Schmutz, S.M. Kaeppler, M.D. Casler, and C.R. Buell. 2015. Diversity and population structure of northern switchgrass as revealed through exome capture sequencing. Plant J. 84(4): 800–815.

Evans, J., J. Kim, K.L. Childs, B. Vaillancourt, E. Crisovan, A. Nandety, D.J. Gerhardt, T.A. Richmond, J.A. Jeddeloh, S.M. Kaeppler, M.D. Casler, and C.R. Buell. 2014. Nucleotide polymorphism and copy number variant detection using exome capture and next-generation sequencing in the polyploid grass Panicum virgatum. Plant J. 79(6): 993–1008.

Fajolu, O.L. 2012. Characterization of Bipolaris species, their effects on switchgrass biomass yield and chemical components.

Fan, Y., & Song, Y. Q. 2016). Finding the missing heritability of genome-wide association study using genotype imputation. Matters, 2(5), e201604000013.

Friesen, T.L., J.D. Faris, P.S. Solomon, and R.P. Oliver. 2008. Host-specific toxins: effectors of necrotrophic pathogenicity. Cell. Microbiol. 10(7): 1421–1428

Friesen, T.L., S.W. Meinhardt, and J.D. Faris. 2007. The Stagonospora nodorum-wheat pathosystem involves multiple proteinaceous host-selective toxins and corresponding host sensitivity genes that interact in an inverse gene-for-gene manner. Plant J. 51(4): 681–692.

Gao, Y., C. He, D. Zhang, X. Liu, Z. Xu, Y. Tian, X.-H. Liu, S. Zang, M. Pauly, Y. Zhou, and B. Zhang. 2017. Two Trichome Birefringence-Like Proteins Mediate Xylan Acetylation, Which Is Essential for Leaf Blight Resistance in Rice. Plant Physiol. 173(1): 470–481.

Geisler, K., R.K. Hughes, F. Sainsbury, G.P. Lomonossoff, M. Rejzek, S. Fairhurst, C.-E. Olsen, M.S. Motawia, R.E. Melton, A.M. Hemmings, S. Bak, A. Osbourn, and J.R. Ecker. Biochemical analysis of a multifunctional cytochrome P450 (CYP51) enzyme required for synthesis of antimicrobial triterpenes in plants. Proceedings of the National Academy of Sciences. 110(35): E3360-E3367.

Gómez-Gómez, L., and T. Boller. 2000. FLS2: an LRR receptor-like kinase involved in the perception of the bacterial elicitor flagellin in Arabidopsis. Mol. Cell 5(6): 1003–11.

Goodstein, D.M., S. Shu, R. Howson, R. Neupane, R.D. Hayes, J. Fazo, T. Mitros, W. Dirks, U. Hellsten, N. Putnam, and D.S. Rokhsar. 2012. Phytozome: a comparative platform for green plant genomics. Nucleic Acids Res. 40(1): 1178–1186.

Grabowski, P.P., J. Evans, C. Daum, S. Deshpande, K.W. Barry, M. Kennedy, G. Ramstein, S.M. Kaeppler, C.R. Buell, Y. Jiang, and M.D. Casler. 2017. Genome-wide associations with flowering time in switchgrass using exome-capture sequencing data. New Phytol. 213(1): 154–169.

Guo, Y., Y. Huang, L. Hou, J. Ma, C. Chen, H. Ai, L. Huang, and J. Ren. 2017. Genome-wide detection of genetic markers associated with growth and fatness in four pig populations using four approaches. Genet. Sel. Evol. 49(1): 21.

Gupta, S.K., A.K. Rai, S.S. Kanwar, and T.R. Sharma. 2012. Comparative analysis of zinc finger proteins involved in plant disease resistance. PLoS One 7(8): e42578.

Idnurm, A., and B.J. Howlett. 2002. Isocitrate lyase is essential for pathogenicity of the fungus *Leptosphaeria maculans* to canola (*Brassica napus*). Eukaryot. Cell 1(5): 719–24.

Jambunathan, N., and T.W. McNellis. 2003. Regulation of Arabidopsis COPINE 1 gene expression in response to pathogens and abiotic stimuli. Plant Physiol. 132(3): 1370–81.

Jorgensen, I.H. 1992. Discovery, characterization and exploitation of Mlo powdery mildew resistance in barley. Euphytica 63(1–2): 141–152.

Juliana, P., R.P. Singh, P.K. Singh, J.A. Poland, G.C. Bergstrom, J. Huerta-Espino, S. Bhavani, J. Crossa, and M.E. Sorrells. 2018. Genome-wide association mapping for resistance to leaf rust, stripe rust and tan spot in wheat reveals potential candidate genes. Theor. Appl. Genet.: 1–18.

Katara, J. L., Sonah, H., Deshmukh, R. K., Chaurasia, R., & Kotasthane, A. S. 2010. Molecular analysis of QTLs associated with resistance to brown spot in rice (Oryza sativa L.). Indian J. Genet. 70(1): 17-21.

Kim, J.Y., J. Wu, S.J. Kwon, H. Oh, S.E. Lee, S.G. Kim, Y. Wang, G.K. Agrawal, R. Rakwal, K.Y. Kang, I.P. Ahn, B.G. Kim, and S.T. Kim. 2014. Proteomics of rice and Cochliobolus miyabeanus fungal interaction: Insight into proteins at intracellular and extracellular spaces. Proteomics 14(20): 2307–2318.

Kumar, M., W. Busch, H. Birke, B. Kemmerling, T. Nürnberger, and F. Schöffl. 2009. Heat shock factors HsfB1 and HsfB2b are involved in the regulation of Pdf1.2 expression and pathogen resistance in Arabidopsis. Mol. Plant 2(1): 152–65.

Lee, M.-W., M. Qi, and Y. Yang. 2001. A Novel Jasmonic Acid-Inducible Rice myb Gene associates with fungal infection and host cell death. Mol. Plant-Microbe Interact. 14(4): 527–535.

Li, D., H. Liu, H. Zhang, X. Wang, and F. Song. 2008. OsBIRH1, a DEAD-box RNA helicase with functions in modulating defense responses against pathogen infection and oxidative stress. J. Exp. Bot. 59(8): 2133–46.

Lipka, A. E., Gore, M. A., Magallanes-Lundback, M., Mesberg, A., Lin, H., Tiede, T., & DellaPenna, D. 2013. Genome-wide association study and pathway level analysis of tocochromanol levels in maize grain. G3: Genes, Genomes, Genetics. g3-113.

Lipka, A.E., F. Lu, J.H. Cherney, E.S. Buckler, M.D. Casler, and D.E. Costich. 2014. Accelerating the switchgrass (Panicum virgatum L.) breeding cycle using genomic selection approaches. PLoS One 9(11): 1–7.

Lu, F., A.E. Lipka, J. Glaubitz, R. Elshire, J.H. Cherney, M.D. Casler, E.S. Buckler, and D.E. Costich. 2013. Switchgrass Genomic Diversity, Ploidy, and Evolution: Novel Insights from a Network-Based SNP Discovery Protocol. PLoS Genet. 9(1).

Mammarella, N.D., Z. Cheng, Z.Q. Fu, A. Daudi, G.P. Bolwell, X. Dong, and F.M. Ausubel. 2015. Apoplastic peroxidases are required for salicylic acid-mediated defense against Pseudomonas syringae. Phytochemistry 112: 110–121.

Martin, E.R., D.D. Kinnamon, M.A. Schmidt, E.H. Powell, S. Zuchner, and R.W. Morris. 2010. SeqEM: an adaptive genotype-calling approach for next-generation sequencing studies. Bioinformatics 26(22): 2803–2810.

Miyakawa, T., K. Miyazono, Y. Sawano, K. Hatano, and M. Tanokura. 2009. Crystal structure of ginkbilobin-2 with homology to the extracellular domain of plant cysteine-rich receptor-like kinases. Proteins Struct. Funct. Bioinforma. 77(1): 247–251.

Muir, W.M. 2007. Comparison of genomic and traditional BLUP-estimated breeding value accuracy and selection response under alternative trait and genomic parameters. J. Anim. Breed. Genet. 124(6): 342–355.

Okada, M., C. Lanzatella, M.C. Saha, J. Bouton, R. Wu, and C.M. Tobias. 2010. Complete

switchgrass genetic maps reveal subgenome collinearity, preferential pairing and multi-locus interactions. Genetics 185(3): 745–760.

Park, C.-J., T. Wei, R. Sharma, and P.C. Ronald. 2017. Overexpression of Rice Auxilin-Like protein, XB21, induces necrotic lesions, up-regulates endocytosis-related genes, and confers enhanced resistance to *Xanthomonas oryzae* pv. oryzae. Rice. 10(1): 27.

Purcell, S., B. Neale, K. Todd-Brown, L. Thomas, M.A.R. Ferreira, D. Bender, J. Maller, P. Sklar, P.I.W. de Bakker, M.J. Daly, and P.C. Sham. 2007. PLINK: A tool set for whole-genome association and population-based linkage analyses. Am. J. Hum. Genet. 81(3): 559–575.

Ralph, S., J.-Y. Park, J. Bohlmann, and S.D. Mansfield. 2006. Dirigent proteins in conifer defense: gene discovery, phylogeny, and differential wound- and insect-induced expression of a family of DIR and DIR-like Genes in spruce (*Picea* spp.). Plant Mol. Biol. 60(1): 21–40.

Sato, H., I. Ando, H. Hirabayashi, Y. Takeuchi, S. Arase, J. Kihara, H. Kato, T. Imbe, and H. Nemoto. 2008. QTL analysis of brown spot resistance in rice (*Oryza sativa* L.). Breed. Sci. 58(1): 93–96.

Sato, H., K. Matsumoto, C. Ota, T. Yamakawa, J. Kihara, and R. Mizobuchi. 2015. Confirming a major QTL and finding additional loci responsible for field resistance to brown spot (Bipolaris oryzae) in rice. Breed. Sci. 65(2): 170–175.

Sawano, Y., T. Miyakawa, H. Yamazaki, M. Tanokura, and K. Hatano. 2007. Purification, characterization, and molecular gene cloning of an antifungal protein from Ginkgo biloba seeds. Biol. Chem. 388(3): 273–80.

Silva, W., J. Ingram, C.A. Hackett, J.J. Coombs, D. Douches, G. Bryan, W. De Jong, and S.

Gray. 2017. Mapping loci that control tuber and foliar symptoms caused by PVY in Autotetraploid Potato (*Solanum tuberosum* L.). Genes Genomes Genetics: g3-300264.

Smit, J.J., and T.K. Sixma. 2014. RBR E3-ligases at work. EMBO Rep. 15(2): 142–54.

Solomon, M., B. Belenghi, M. Delledonne, E. Menachem, and A. Levine. 1999. The involvement of cysteine proteases and protease inhibitor genes in the regulation of programmed cell death in plants. Plant Cell 11(3): 431–44.

Songsomboon, K., R. Crawford, J. Crawford, J. Hansen, J. Cummings, N. Mattson, G. Bergstrom, D. Viands. 2018. Recurrent phenotypic selection for resistance to diseases caused by Bipolaris oryzae in switchgrass (*Panicum virgatum*). Manuscript submitted for publication.

Stein, M., J. Dittgen, C. Sánchez-Rodríguez, B.-H. Hou, A. Molina, P. Schulze-Lefert, V. Lipka, and S. Somerville. 2006. Arabidopsis PEN3/PDR8, an ATP binding cassette transporter, contributes to nonhost resistance to inappropriate pathogens that enter by direct penetration. Plant Cell 18(3): 731–46.

Stewart, E.L., and B.A. McDonald. 2014. Measuring quantitative virulence in the wheat pathogen *Zymoseptoria tritici* using high-throughput automated image analysis. Phytopathology 104(9): 985–992.

Stroup, J., M. Sanderson, J.P. Muir, M.J. McFarland, and R.L. Reed. 2003. Comparison of growth and performance in upland and lowland switchgrass types to water and nitrogen stress. Bioresour. Technol. 86: 65–72.

Tsuchiya, T., and T. Eulgem. 2011. EMSY-Like Genes Are Required for Full RPP7-Mediated Race-Specific Immunity and Basal Defense in Arabidopsis. 24(1210): 1573–1581.

Tsuchiya, T., and T. Eulgem. 2013. An alternative polyadenylation mechanism coopted to the

Arabidopsis RPP7 gene through intronic retrotransposon domestication. Proc. Natl. Acad. Sci. U. S. A. 110(37): E3535-43.

Walter, S., A. Kahla, C. Arunachalam, A. Perochon, M.R. Khan, S.R. Scofield, and F.M. Doohan. 2015. A wheat ABC transporter contributes to both grain formation and mycotoxin tolerance. J. Exp. Bot. 66(9): 2583–2593.

Xue, D., Q. Wang, Z. Chen, L. Cai, L. Bao, Q. Qi, L. Liu, X. Wang, H. Jin, J. Wang, H. Wu, H. Liu, and Q. Chen. 2015. 3-Anhydro-6-hydroxy-ophiobolin A, a fungal sesterterpene from Bipolaris oryzae induced autophagy and promoted the degradation of α-synuclein in PC12 cells. Bioorg. Med. Chem. Lett. 25(7): 1464–1470.

Yaeno, T., O. Matsuda, and K. Iba. 2004. Role of chloroplast trienoic fatty acids in plant disease defense responses. Plant J. 40(6): 931–941.

You, Q., K. Zhai, D. Yang, W. Yang, J. Wu, J. Liu, W. Pan, J. Wang, X. Zhu, Y. Jian, J. Liu, Y. Zhang, Y. Deng, Q. Li, Y. Lou, Q. Xie, and Z. He. 2016. An E3 Ubiquitin Ligase-BAG protein module controls plant innate immunity and broad-spectrum disease resistance. Cell Host Microbe 20(6): 758–769.

Zhao, K., C. W. Tung, G.C. Eizenga, M.H. Wright, M.L. Ali, A.H. Price, G.J. Norton, M.R. Islam, A. Reynolds, J. Mezey, A.M. McClung, C.D. Bustamante, and S.R. McCouch. 2011. Genome-wide association mapping reveals a rich genetic architecture of complex traits in Oryza sativa. Nat. Commun. 2: 467.

Zhou, X., and M. Stephens. 2012. Genome-wide efficient mixed-model analysis for association studies. Nat. Genet. 44(7): 821–4.

TABLES

Table 1. Broad-sense heritability (s.e.) of each trait.

Traits	**H (s.e.)**
Severity from the leaf detachment via vision (DTVI)	0.76 ± 0.02
Severity from the leaf detachment via image analysis (DTIA)	0.74 ± 0.06
Severity from the leaf disk assay via vision (DSVI)	0.56 ± 0.05
Severity from the leaf disk assay via image analysis (DSIA)	0.54 ± 0.04
BLUPs two locations	0.003 ± 0.06
BLUPs NY	0.32 ± 0.05
BLUPs PA	0.61 ± 0.04

780 Table 2. Markers significantly associated with resistance in each case.

Cases	SNP	Chro-mo-some	Dis-tance from gene (bp)	p-value	*P. virgatum* gene	Orthologous genes	Identity	Predicted function
479-DTIA-DSIA-MNY	snp151084	Chr02a	419	1.32E-06	Pavir.Ba03861.1	Pahal.B02018.1[Pha]	99.4	copper transport protein ATOX1-related
	snp680175	Chr02b	975	3.17E-06	Pavir.Bb02195.1	Pahal.B02834.1[Pha]	94.8	E3 ubiquitin-protein ligase RNF144 [EC:6.3.2.19]
			3533		Pavir.Bb02196.1	Pahal.J00890.1[Pha]	93.8	RBR family ring finger and IBR domain-containing
	snp359167	Chr06a	2850	2.96E-06	Pavir.Fa00433.1 Pavir.Fa00433.2	Pahal.F00718.1[Pha]	88.9	ENT domain
			716		Pavir.Fa00434.1	Pahal.F00719.1[Pha]	70.9	Myb-like DNA- binding domain, Bromodomain
			2690		Pavir.Fa00435.1	Pahal.F00721.1[Pha]	54.6	uncharacterized C-terminal mem-brane protein
			8477		Pavir.Fa00437.1	LOC_Os04g48030.1[Osa]	8.5	heat stress transcription factor B-1
	snp933838	Chr07b	1453	2.12E-06	Pavir.Gb01298.1 Pavir.Gb01298.2	Sobic.006G139100.1[Sbi]	96.7	polyadenylate-binding protein
			609		Pavir.Gb01299.1	Pahal.H00668.1[Pha]	93.5	2,3-dimethylmalate lyase, (2R,3S)-2,3-dimethylmalate py-ruvate-lyase, isocitrate lyase
	snp938364	Chr07b	597	6.81E-06	Pavir.Gb01488.1* Pavir.Gb01488.2*	LOC_Os04g39430.1[Osa]	85.6	cytochrome P450
			2987		Pavir.Gb01489.1 Pavir.Gb01489.2	Pahal.G00545.1[Pha]	97.4	protection of telomeres 1

Cases	SNP	Chro-mo-some	Dis-tance from gene (bp)	p-value	*P. virgatum* gene	Orthologous genes	Identity	Predicted function
					Pavir.Gb01489.3 Pavir.Gb01489.4			
	snp465249	Chr09a	3464	1.58E-07	Pavir.Ia00174.1	Pahal.I01213.1[Pha]	97.3	protein trichome Birefringence-like 32
			1915		Pavir.Ia00175.1 Pavir.Ia00175.2	Sobic.001G038100.1[Sbi]	92.2	protein FLC expressor
	snp469523	Chr09a	5412	4.77E-06	Pavir.Ia00350.2	Pahal.I01603.1[Pha]	89.4	protein K03B8.4-related
			2256	4.77E-06	Pavir.Ia00351.1	Sobic.001G079200.1[Sbi]	97.3	mitogen-activated kinase kinase kinase (MAP)
	snp1003871	Chr09b	5314	9.85E-06	Pavir.Ib01315.1 Pavir.Ib01315.2	Sevir.9G450400.1[Svi]	95.0	glutathione s-transferase (GST)
			788		Pavir.Ib01317.1	Pahal.I04479.1[Pha]	94.1	glutathione s-transferase (GST)
			3573		Pavir.Ib01318.1	Zm00008a00114T01[Zma]	83.0	ent-kaurenoic acid hydroxylase (KAO) subfamily P450
4X-MNYNY	snp316732	Chr05a	8347	6.08E-07	Pavir.Ea02827.1	Sevir.3G000300.1[Svi]	63.6	Actinidain/Actinidin [3.4.22.14], cysteine protease, Cathepsin pro-peptide inhibitor domain
			2009		Pavir.Ea02828.1 Pavir.Ea02828.2 Pavir.Ea02828.3	Pahal.E01498.1[Pha]	96.3	[3.64.13] RNA helicase, ATP-de-pendent RNA helicase, DEAD/DEAH box helicase
	snp444058	Chr08a	1739	1.21E-06	Pavir.Ha00272.1	Pahal.H00237.1[Pha]	90.6	auxilin/cyclin g-associated ki-nase-related
low-	snp594527	Chr01b	7186	2.37E-06	Pavir.Ab01193.1 Pavir.Ab01193.2 Pavir.Ab01193.3	LOC_Os07g35340.1[Osa]	74.7	protein kinase domain (Pkinase), salt stress response,antifungal (stress-antifung)

Cases	SNP	Chro-mo-some	Dis-tance from gene (bp)	p-value	*P. virgatum* gene	Orthologous genes	Identity	Predicted function
			199		Pavir.Ab01194.1	Pahal.A00997.1[Pha]	56.0	component of root nitrate treat-ment specific coexpression sub-network
	snp197006	Chr03a	1106	1.58E-06	Pavir.Ca02197.1	Sobic.008G093000.1[Sbi]	92.6	ATP-binding cassette (ABC) transporter
	snp732235	Chr03b	1613	1.75E-06	Pavir.Cb01411.1 Pavir.Cb01411.2	Zm00008a03100T01[Zma]	99.8	elongation factor 1-alpha (EEF1A)
			4102		Pavir.Cb01412.1	Sobic.009G118300.1[Sbi]	95.1	copine
	snp791318	Chr05b	7974	2.56E-09	Pavir.Eb00172.1	Sevir.5G014600.1[Svi]	82.6	protein kinase domain (Pkinase), S-locus glycoprotein domain, D-mannose binding lectin (B_lec-tin), PAN-like domain (PAN_2), serine/threonine protein kinase
			5076		Pavir.Eb00173.1 Pavir.Eb00173.2	Pahal.E04515.1[Pha]	97.7	HAT family dimerization do-main-containing protein, BED zinc finger
			1362		Pavir.Eb00174.1	Pahal.E04517.1[Pha]	98.3	Diacylglycerol o-acyltransferase 1 (DGAT1)
			2273		Pavir.Eb00175.1	Sobic.003G013800.1[Sbi]	88.0	uncharacterized
	snp791375	Chr05b	3373	4.16E-06	Pavir.Eb00177.1	Sobic.003G014100.1[Sbi]	64.8	GDT1-like protein 1, chloro-plastic, membrane protein
			4141		Pavir.Eb00178.1	Sobic.003G014300.2[Sbi]	99.5	Snoal-like domain, uncharacter-ized conserved protein
up-	snp411929	Chr07a	2184	3.44E-07	Pavir.Ga00855.1 Pavir.Ga00855.2 Pavir.Ga00855.3	Pahal.G01363.1[Pha]	96.8	RNA polymerase II, C-terminal domain phosphatase-like 1/2

Cases	SNP	Chro-mo-some	Dis-tance from gene (bp)	p-value	*P. virgatum* gene	Orthologous genes	Identity	Predicted function
								[EC:3.1.3.16] (CPL1_2), protein-serine/threonine phosphatase
			6254		Pavir.Ga00856.1	Zm00008a03828T01[Zma]	74.2	lactosylceramide 4-alpha-galacto-syltransferase
	snp411995	Chr07a	2093	8.66E-07	Pavir.Ga00857.1	Sobic.006G156600.2[Sbi]	97.2	transporter family protein
			507		Pavir.Ga00858.1	Sobic.006G156600.2[Sbi]	54.0	sugar (and other) transporter
			49		Pavir.Ga00859.1 Pavir.Ga00859.2 Pavir.Ga00859.3 Pavir.Ga00859.4 Pavir.Ga00859.5 Pavir.Ga00859.6	Zm00008a00013T01[Zma]	76.8	general transcription factor 3c polypeptide 6 (GTF3C6)
			6080		Pavir.Ga00860.1 Pavir.Ga00860.2	Zm00008a00671T01[Zma]	92.2	expansin precursor
	snp412960	Chr07a	673	3.08E-06	Pavir.Ga00912.1 Pavir.Ga00912.2	Sobic.006G156300.1[Sbi]	92.7	WD-40 repeat family protein

* *P. virgatum* genes that overlapping with resistance genes in *Oryza sativa* search

[Osa] gene from *Oryza sativa*

[Pha] gene from Panicum hallii

[Sbi] gene from Sorghum bicolor

[Svi] gene from Setaria viridis

[Zma] gene from Zea may

Table 3 Phenotypic variance explained (PVE) (adjusted PVE) by accumulative 18 significant SNP markers across all analyses for each trait.

Traits	PVE (adjusted PVE)
DTVI	7.68 (4.07)
DTIA	6.32 (2.65)
DSIA	26.72 (23.85)
MNY	9.93 (6.4)
MPA	11.38 (7.91)

Abbreviation: BLUPs of severity from the leaf detachment via vision (DTVI), BLUPs of severity from the leaf detachment via image analysis (DTIA), BLUPs of severity from the leaf disk assay via image analysis (DSIA), highest score of BLS in NY (MNY), highest score of BLS in PA (MPA).

FIGURES

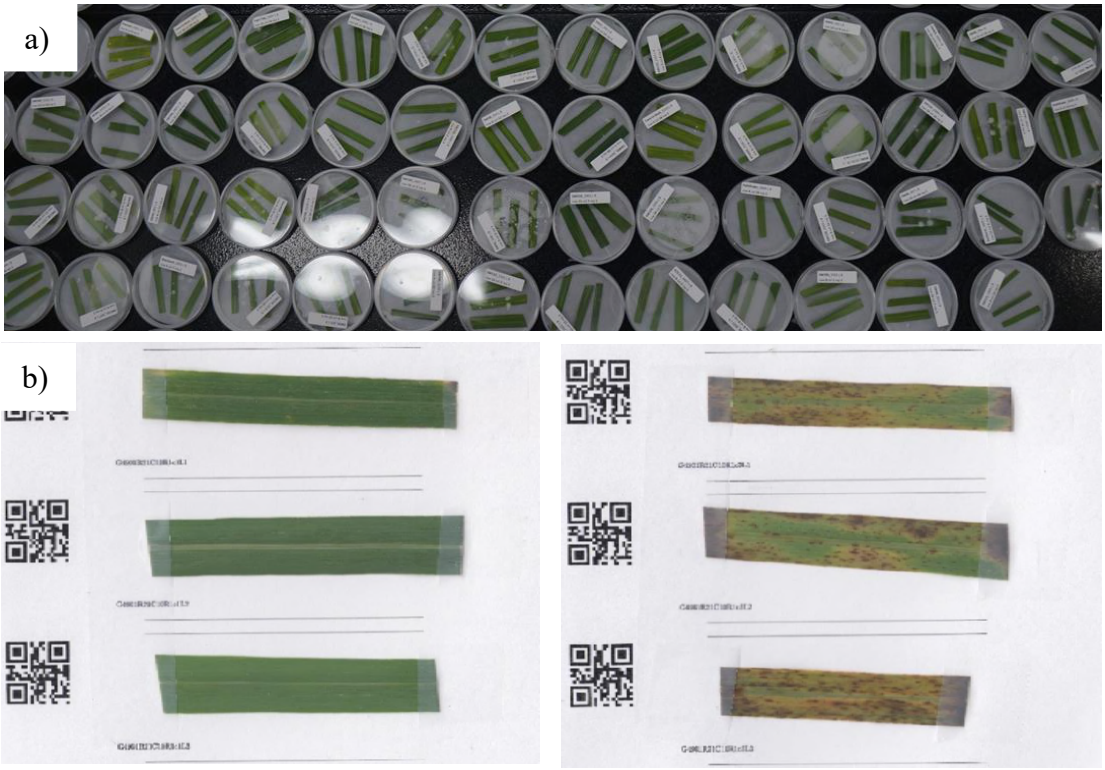

Figure 1. Leaf detachment assay; a) sealed plates of detached leaves under 24-h light 25°C; b) control inoculated (left) and inoculated leaves (right) at 7 dpi were taped on white paper with QR code label for scanning for image analysis.

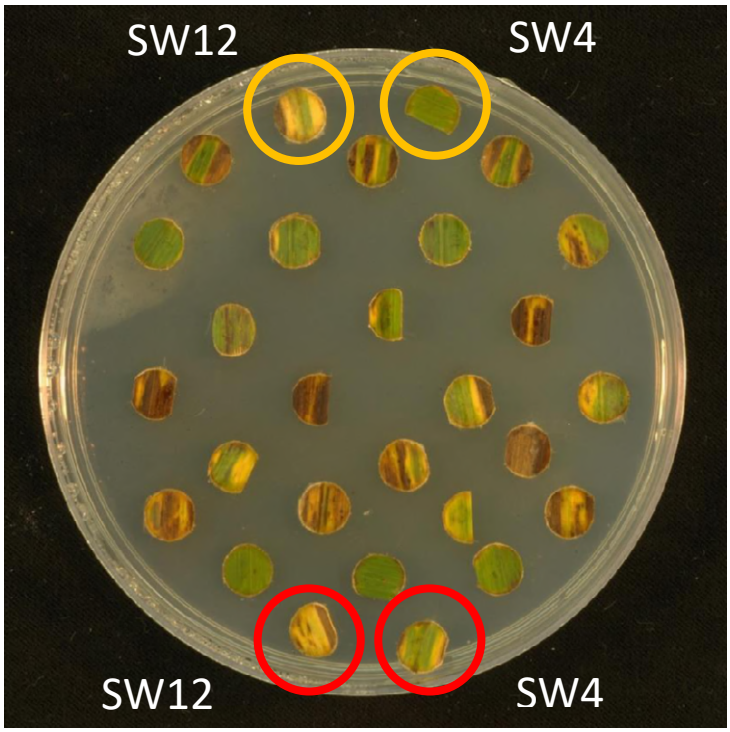

Figure 2. A plate example of leaf disk assay at 7 dpi. Each plate consisted of 28 leaf disks. SW43_09 was used as a resistant check and SW122_02 as a susceptible check. Two control leaf disks (yellow circles) and two inoculated leaf disks (red circles) were included in all plates. The rest of the leaf disks (24) consisted of eight genotypes with three replicates placed in a consecutive row from left to right.

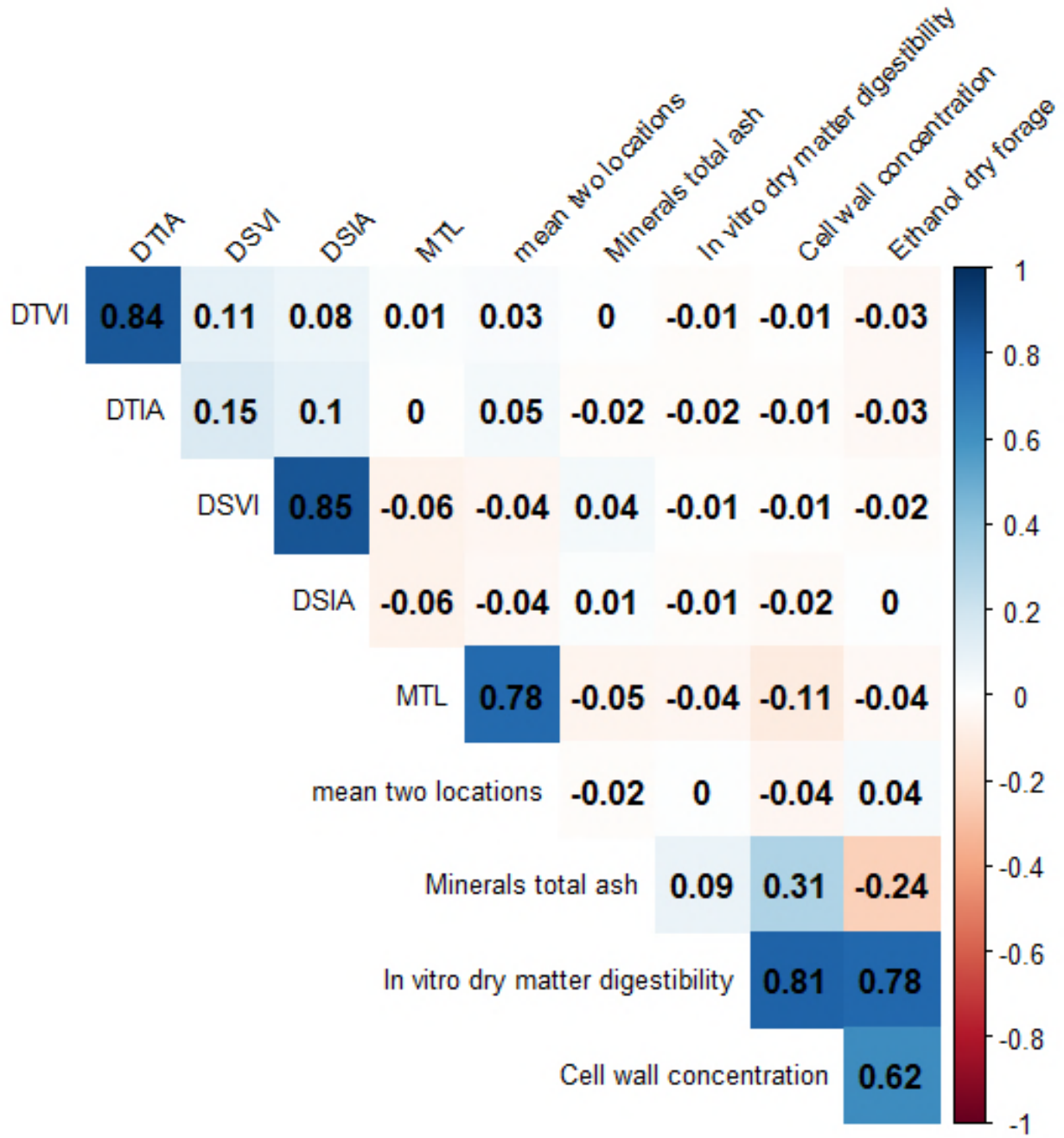

Figure 3. Correlation plot among BLUPs of severity from the leaf detachment via vison (DTVI), via image analysis (DTIA), from leaf disk assay via vision (DSVI), via image analysis (DSIA), the highest score between two locations (MTL), mean from two location, minerals total ash, *in vitro* dry matter digestibility, and cell wall concentration.

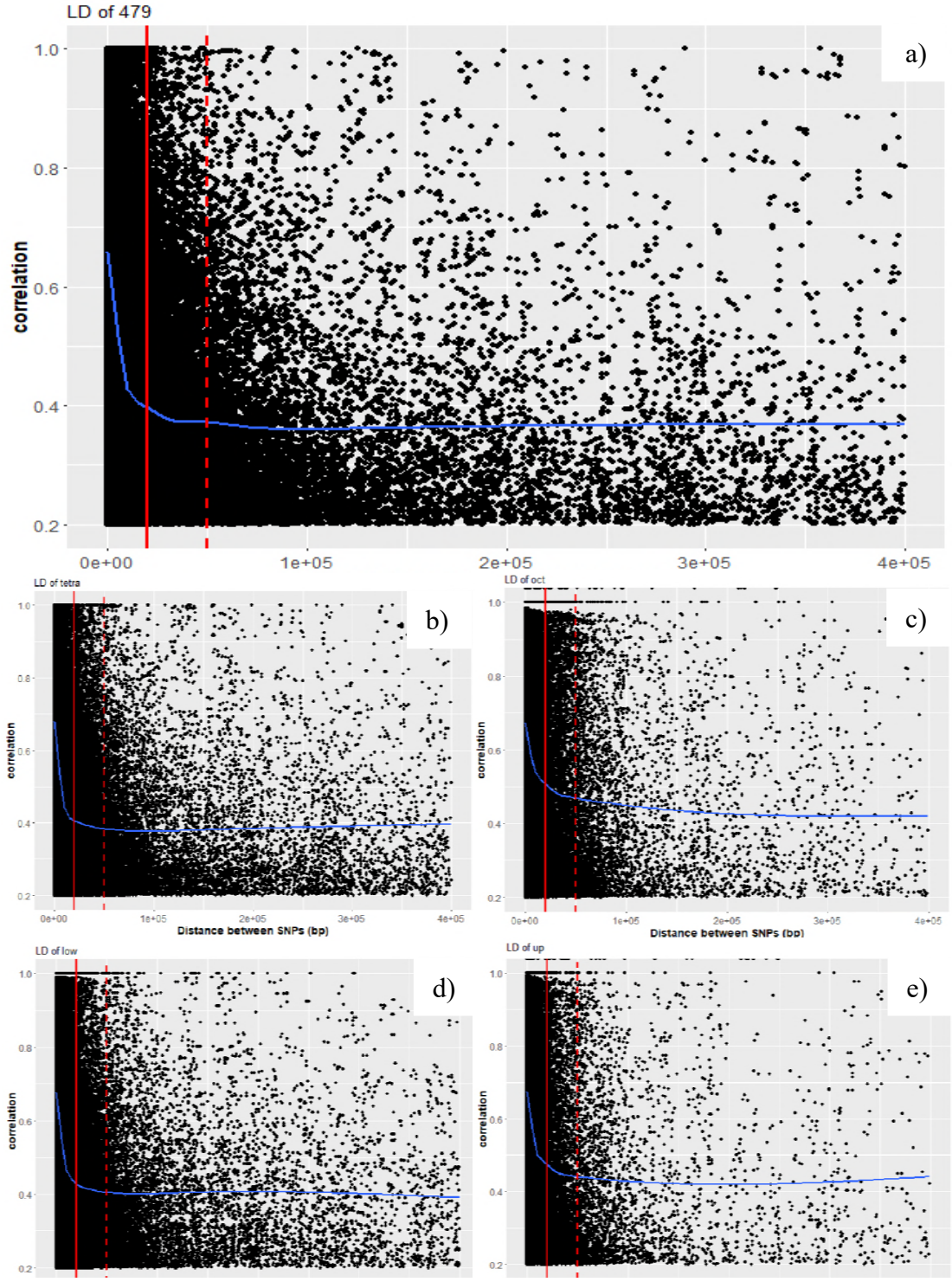

Figure 4. Scatter plot showing the linkage disequilibrium (LD) decay by plotting physical distance in base pairs against the LD estimate as correlation (R^2) in a) 479 genotypes, b) 4X group, c) 8X group, d) lowland ecotype, and e) upland ecotype. From full set of 479 genotypes, the LD (blue curve) decays rapidly within 20 kb (red line) and reaches background levels around 50 kb (dashed red line).

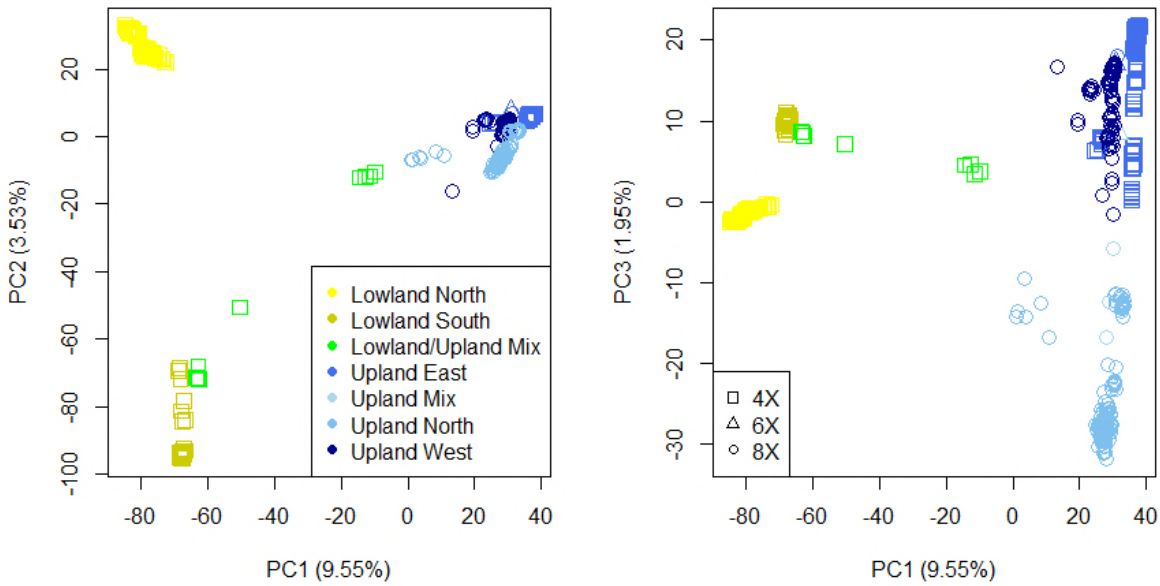

Figure 5. The 479 switchgrass genotypes from the Northern Association Panel showing the different distributions based on ecotype and region from principal component analysis (PC). The lowland ecotype can be differentiated into two regions from PC1 and PC2, and the upland ecotype can be grouped into three regions from PC1 and PC3.

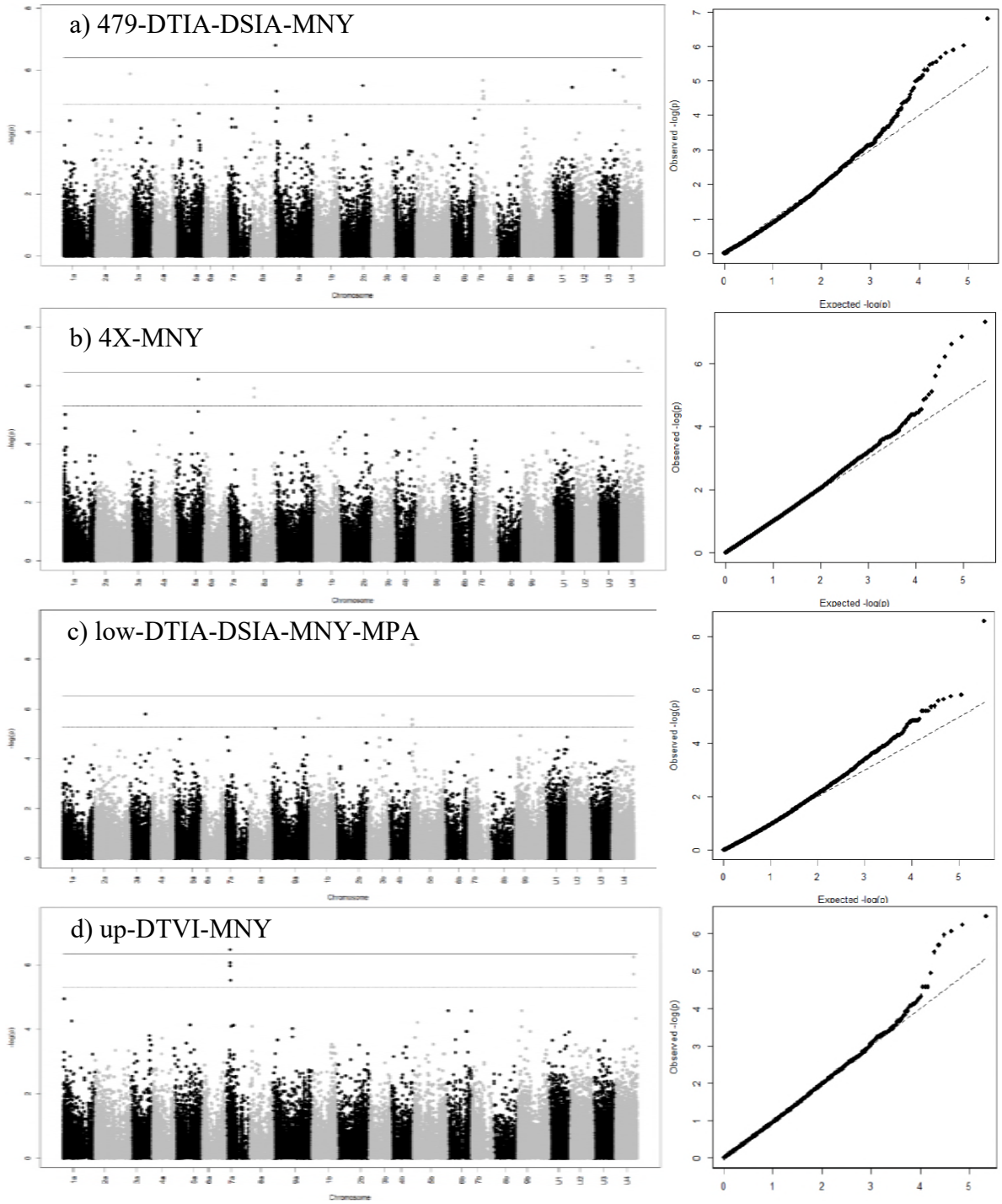

Figure 6. (Left) Manhattan plot showing genetic associated of a) DTIA-DSIA-MNY in 479 genotypes, b) MNY in 4X genotypes, c) DTIA-DSIA-MNY-MPA in lowland ecotype and d) DTVI-MNY in upland genotypes. The dashed line represents the FDR threshold (0.1) and the line represents Bonferroni correction threshold. On x-axis, the physical positions of the SNPs were aligned in 18 chromosomes of *P. virgatum*; however, there were 16,676 genes that cannot be assigned to the genome and noted as chromosome U1-U4. (right) Quantile-quantile (QQ) plots between the distributions of observed to expected P-values for GWAS of each trait combination in each genotype group.

Abbreviation: BLUPs of severity from the leaf detachment via vision (DTVI), BLUPs of severity from the leaf detachment via image analysis (DTIA), BLUPs of severity from the leaf disk assay via image analysis (DSIA), highest score of BLS in NY (MNY), highest score of BLS in PA (MPA).